In-Phase and Anti-Phase Power Dividers for UWB Differentially Fed Antenna Arrays

Mario Leib, *Student Member, IEEE*, Andreas Vollmer, and Wolfgang Menzel, *Fellow, IEEE*

***Abstract*—This letter presents two novel power dividers operating in the FCC frequency range from 3.1 to 10.6 GHz. The two outputs of each power divider are coplanar striplines, while the input is a microstrip line. Hence, the power dividers act as baluns and are suited for differentially fed antennas. The in-phase version shows a return loss of better than 15 dB from 1 to 12.3 GHz, whereas for the anti-phase version the return loss is better than 10 dB from 1 to 12.3 GHz. Besides the characterization of the dividers, a linear antenna array fed by one of the dividers is shown, and measurement results in the time domain and frequency domain are presented. The mean gain of the realized four-element array is 9.7 dBi.**

***Index Terms*—Antenna array feeds, coplanar transmission lines, microstrip transitions, power dividers, ultrawideband (UWB).**

I. Introduction

ULTRAWIDEBAND (UWB) antenna arrays are of interest in various applications, e.g., in ground-penetrating radars for land mine detection [1] or in the medical environment for breast cancer detection [2] and patient monitoring [3]. The high directivity obtained by array arrangements combined with the high-resolution capabilities of UWB technology leads to outstanding system performances. In addition, an array gives the opportunity to avoid mechanical scanning applying beam steering [4].

Differentially fed antennas are preferred since they are resistant to cable currents and the low radiation of feeding lines. Hence, the radiation pattern is not affected by these parasitic influences. Additionally, differentially fed arrays offer low element coupling and low cross polarization [5]. In combination with differential monolithically integrated circuits (MMICs), differentially fed antennas are preferred because no lossy baluns are required, leading to compact systems.

Depending on the layout of the single antenna and the element placement, in-phase or anti-phase feeding structures are needed to achieve a constructive superposition of the radiated electromagnetic field in the main beam direction. In this letter, novel planar in-phase and anti-phase power dividers with differential outputs are presented. These power dividers are applied to feed a UWB antenna array.

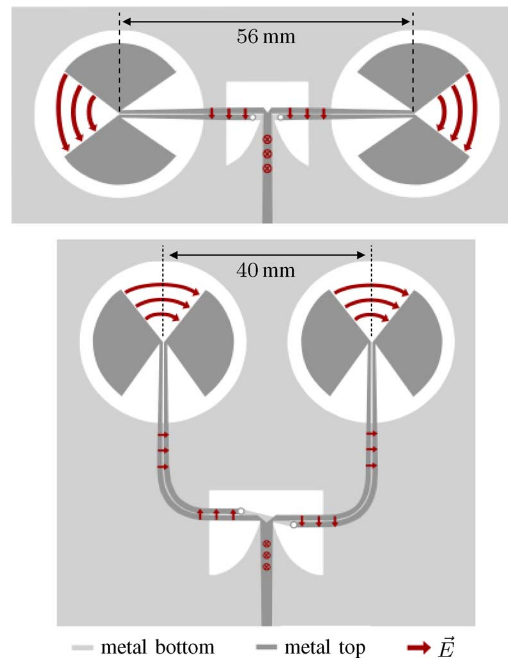

Fig. 1. Sketch of two arrays with a linear array arrangement in the H-plane (top) and the E-plane (bottom) of the antenna.

II. Design of the Power Dividers

The basic concept of the power dividers is a T-junction of a tapered microstrip line (MSL) with two coplanar striplines (CPS). The transition to the CPS is achieved using a vertical through connection (via) and leads to a fractional bandwidth of more than 170%. A similar power divider was proposed in [6], but radial stubs instead of vias are used, resulting in a bandwidth of only 70%.

In Fig. 1, two antenna arrays are shown fed via in-phase (top) and anti-phase (bottom) power dividers, whereas a circular slot antenna is used as the antenna [7]. The in-phase power divider leads to a constructive superposition of the radiated electrical fields for the array in the H-plane, while a constructive superposition is achieved with the anti-phase divider in the E-plane arrangement. Both dividers and the antennas are designed on the substrate material RO4003 ($\varepsilon_{\rm r} = 3.38$) with a thickness of 0.81 mm using Microwave Studio [8].

A. In-Phase Power Divider

Fig. 2 shows the realized in-phase structure and a sketch of the layout. The impedance of the microstrip line is 50 Ω, while the

Manuscript received April 07, 2010; accepted May 08, 2010. Date of publication May 18, 2010; date of current version May 31, 2010. This work was supported by the Deutsche Forschungsgemeinschaft (DFG) within the priority program UKoLoS.

The authors are with the Institute of Microwave Techniques, University of Ulm, 89081 Ulm, Germany (e-mail: mario.leib@uni-ulm.de; wolfgang.menzel@uni-ulm.de).

Color versions of one or more of the figures in this letter are available online at http://ieeexplore.ieee.org.

Digital Object Identifier 10.1109/LAWP.2010.2050571

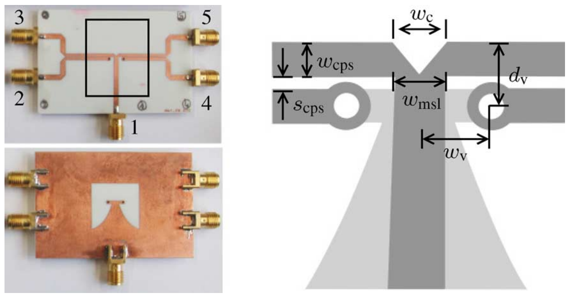

Fig. 2. Fabricated in-phase power divider and sketch of the T-junction.

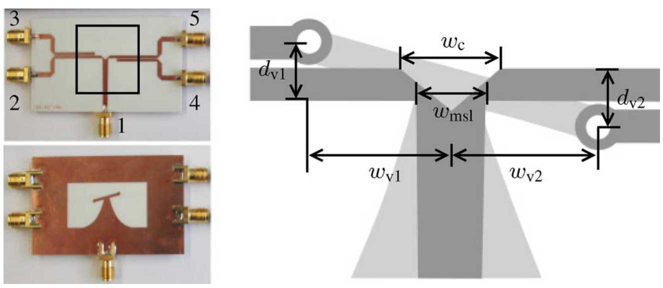

Fig. 3. Fabricated anti-phase power divider and sketch of the T-junction.

TABLE I
DIMENSIONS OF THE IN-PHASE POWER DIVIDER

w_c	w_{msl}	w_v	d_v	w_{cps}	s_{cps}
1.6 mm	1.6 mm	2.7 mm	1.8 mm	1.0 mm	0.3 mm

TABLE II
DIMENSIONS OF THE ANTI-PHASE POWER DIVIDER

w_c	w_{msl}	$w_{v,1}$	$w_{v,2}$	$d_{v,1}$	$d_{v,2}$
3.6 mm	2.3 mm	4.9 mm	5.2 mm	1.8 mm	1.8 mm

impedance of the coplanar striplines is 100 Ω due to the compatibility with differential ICs. All dimensions of the power divider can be found in Table I. The two vias for the vertical interconnection have a diameter of 0.8 mm, and the via pad diameter is 1.2 mm. Simulations showed that slight variations of the via position are not critical.

B. Anti-Phase Power Divider

In contrast to the in-phase structure, the position of the vias are point-symmetrical regarding the T-junction to obtain a phase difference of 180° between both CPS lines. In order to achieve a good transmission at high frequencies, the vias have different distances to the feeding line and are further away from the center of the microstrip line compared to the in-phase power divider. Fig. 3 shows the realized structure and a sketch of the main part, while Table II lists all dimensions.

III. Measurement Results for the Power Dividers

The measured return loss for the in-phase power divider, shown in Fig. 4, is better than 15 dB from 1 to 12.3 GHz and agrees well with the simulation. For characterization of the transmission performance, the coplanar striplines are split into

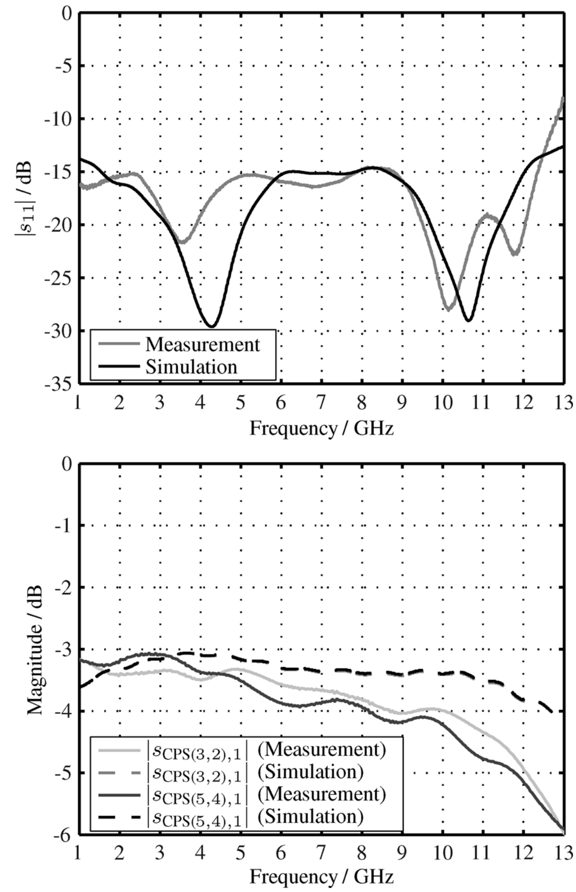

Fig. 4. Return loss (top) and insertion loss (bottom) of the in-phase power divider. Due to symmetry, the simulated insertion loss is identical for both ports.

two separate microstrip lines in the test structure, offering easier single-ended measurements (cf. Figs. 2 and 3). The transmission from the single-ended input port (1) to the differential CPS output ports (2, 3 and 4, 5) is calculated by the single-ended S-parameters using the following equation:

$$\left|s_{\mathrm{CPS}(i,j),1}\right|^2 = |s_{i,1}|^2 + |s_{j,1}|^2. \quad (1)$$

There, i and j denote the microstrip output ports belonging to the respective CPS. In the simulations, the transitions from the CPS to two MSLs, required for the measurement, are included, and the material losses are neglected. This leads to a good agreement for the obtained transmission behavior (see Fig. 4). The power is equally divided between the two output ports with an insertion loss less than 4.6 dB in the frequency band from 3.1 to 10.6 GHz. The observed ripple is caused by reflections at the coaxial connectors. For the anti-phase power divider, the reflection and transmission behaviors are depicted in Fig. 5. The return loss is better than 10 dB from 1 to 12.3 GHz. The power division is slightly unequal due to the asymmetrical layout. If the power dividers are operated differentially, that means without the transition to two MSLs, slightly better results are achieved.

In Fig. 6 the phase differences of the single-ended ports of the respective CPS of both power dividers are shown. Ideally, the phase shift between two related ports is 180°. A deviation of ±8° is obtained in the FCC band with no offset in the case of the in-phase, and an offset of 8° for the anti-phase structure.

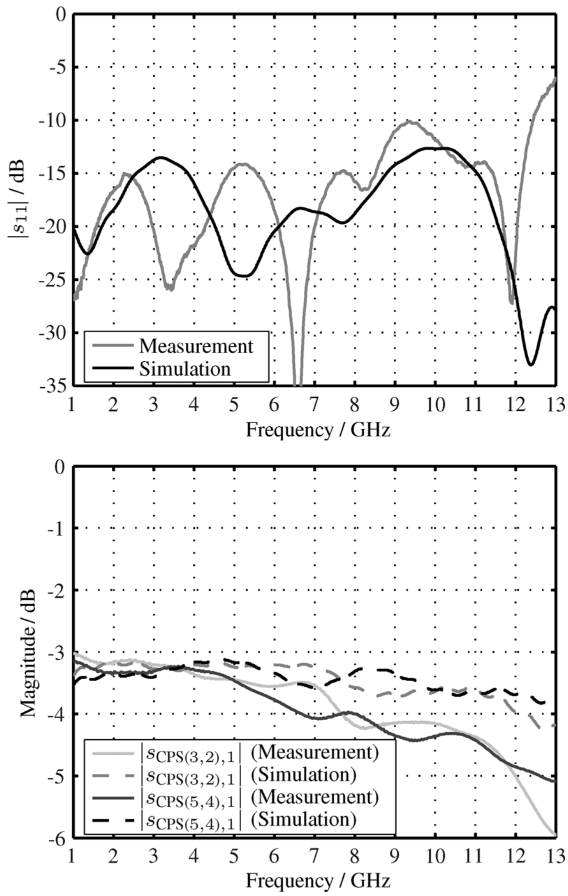

Fig. 5. Return loss (top) and insertion loss (bottom) of the anti-phase power divider.

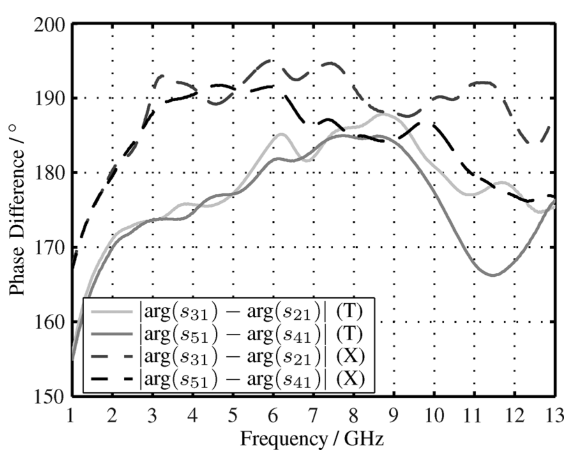

Fig. 6. Measured phase difference of the output ports for the in-phase (T) and anti-phase (X) power divider.

IV. Application on Differentially Fed Circular Slot Antenna

The in-phase power divider was applied to build a four-element antenna array as displayed in Fig. 7. The array consists of two separate subarrays, each fed by a power divider (cf. Fig. 1). Differentially fed slot antennas were chosen as array elements due to their low radiation for $\pm 90°$ leading to a low mutual coupling. The distance between the equally spaced elements is 56 mm. This distance is determined by the antenna dimension

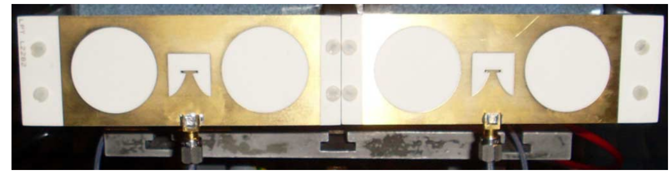

Fig. 7. Realized linear array with four differentially fed circular slot antennas.

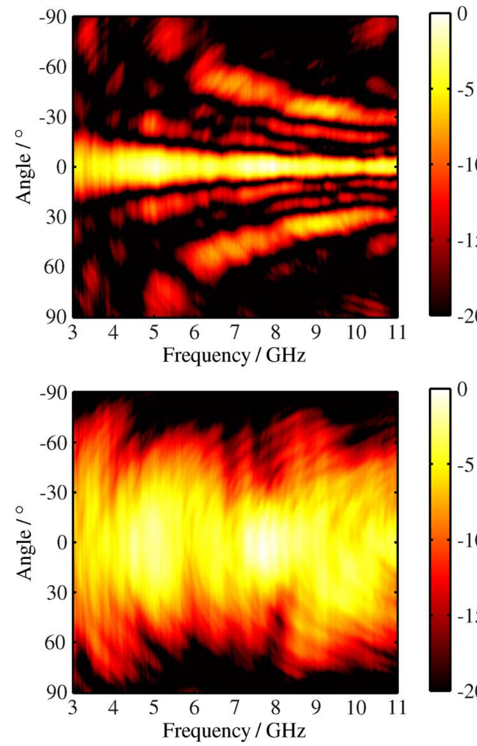

Fig. 8. Measured radiation pattern for the H-plane (top) and E-plane (bottom) of the linear array with four elements.

itself and the required power divider acting also as balun. A smaller distance of 40 mm defined exclusively by the antenna dimensions is possible applying the anti-phase divider (see Fig. 1). The two subarrays are combined by a separate multistage UWB Wilkinson power divider in microstrip technique. The return loss including the Wilkinson power divider is better than 8.8 dB in the FCC band.

The measured radiation pattern in Fig. 8 shows the expected increased directivity in the H-plane, while the E-plane measurement shows the radiation pattern of the single element. The antenna gain has its maximum of 13.3 dBi at 7.7 GHz and a mean value of 9.7 dBi between 3.1 and 10.6 GHz. In the H-plane, grating lobes occur since the element distance is greater than λ for frequencies above 5.3 GHz. Since the positions of the grating lobes are not constant over frequency, the antenna is still suitable for UWB applications. This will be confirmed with the subsequent considerations in the time domain.

The transient response of the array can be calculated from the measured radiation performance using the Fourier transform [9] and is shown in Fig. 9. In the H-plane, the impulse response is focused between $\pm 10°$. In the E-plane, the characteristic of a single element is obtained. The characteristic parameters of the impulse response are the full-width at half-maximum (FWHM)

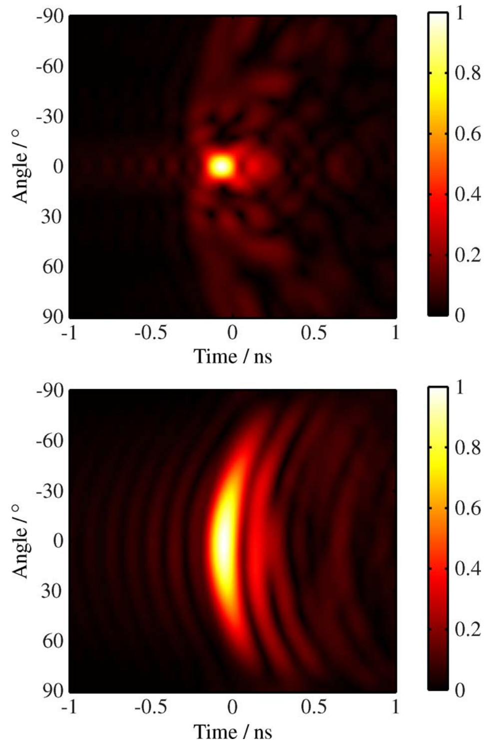

Fig. 9. Normalized envelope of the impulse response obtained by Fourier transformation for the H-plane (top) and E-plane (bottom).

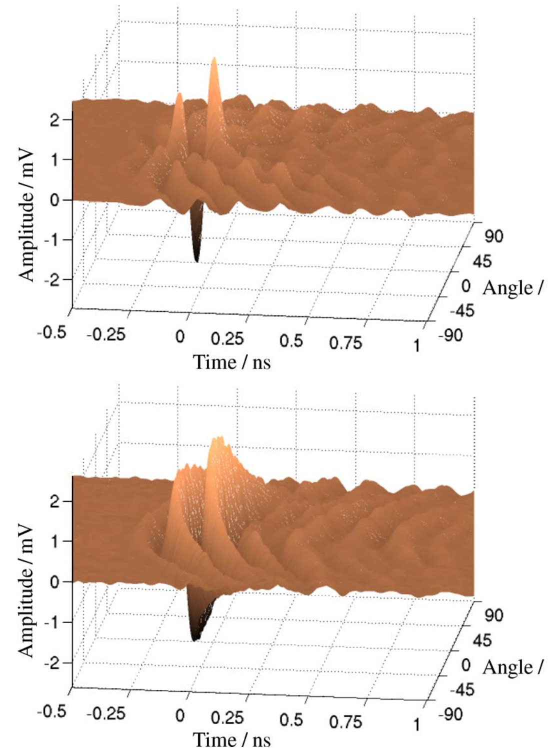

Fig. 10. Measured receive signal for the H-plane (top) and E-plane (bottom).

and the ringing [9]. For the main beam direction, a low FWHM of 134 ps and a low ringing of 0.68 ns is obtained.

The calculated impulse response of the array is verified by the transmission of a real impulse. To this end, the array is fed with an FCC compliant impulse with the shape of a 5th-derivative Gaussian impulse [10]. The radiated and received impulse using a UWB horn antenna for transmitting and a link distance of about 6 m is presented in Fig. 10 for both planes. On the receive side, the impulse is captured by a 12-GHz digital storage oscilloscope. In both planes, a good agreement between the impulse response obtained by the Fourier transform and the time-domain measurement is obvious. In the H-plane, the splitting of the main impulse into four single impulses for high observation angles is clearly visible in this illustration. The splitting is caused by increasing delays between each element for increasing observation angles.

V. Conclusion

In this letter, two novel power dividers are presented, which are suited for differentially fed antennas. The dividers are able to provide good matching and constant power division from 1 to 12.3 GHz. On basis of the in-phase divider, an array has been built and evaluated in frequency and time domain. The time-domain measurements confirm the usage of the array for impulse-based UWB systems.

References

[1] Y. Yang, C. Zhang, S. Lin, and A. Fathy, “Development of an ultra wideband Vivaldi antenna array,” in *Proc. IEEE Int. Antennas Propag. Symp.*, Jul. 2005, vol. 1A, pp. 606–609.

[2] M. Klemm, I. Craddock, J. Leendertz, A. Preece, and R. Benjamin, “Radar-based breast cancer detection using a hemispherical antenna array,” *IEEE Trans. Antennas Propag.*, vol. 57, no. 6, pp. 1692–1704, Jun. 2009.

[3] M. Leib, W. Menzel, B. Schleicher, and H. Schumacher, “Vital signs monitoring with a UWB radar based on a correlation receiver,” presented at the EuCAP, Apr. 2010.

[4] W. Sörgel, C. Sturm, and W. Wiesbeck, “Impulse responses of linear UWB antenna arrays and the application to beam steering,” in *Proc. IEEE ICUWB*, Sep. 2005, pp. 275–280.

[5] E. Pancera, T. Zwick, and W. Wiesbeck, “Differentially fed array for UWB radar applications,” in *Proc. EuCAP*, Mar. 2009, pp. 813–816.

[6] Y.-H. Suh and K. Chang, “Microstrip fed coplanar stripline tee junction using coupled coplanar stripline,” in *Proc. IEEE Int. Microw. Theory Tech. Symp.*, Jun. 2001, vol. 2, pp. 611–614.

[7] M. Leib, M. Frei, and W. Menzel, “A novel ultra-wideband circular slot antenna excited with a dipole element,” in *Proc. IEEE ICUWB*, Sep. 2009, pp. 386–390.

[8] “CST-Computer Simulation Technology”. Microwave Studio, 2009.

[9] W. Sörgel and W. Wiesbeck, “Influence of the antennas on the ultra-wideband transmission,” *EURASIP J. Appl. Signal Process.*, vol. 2005, no. 3, pp. 296–305, 2005.

[10] J. Dederer, B. Schleicher, F. A. T. Santos, A. Trasser, and H. Schumacher, “FCC compliant 3.1–10.6 GHz UWB pulse radar using correlation detection,” in *Proc. IEEE Int. Microw. Theory Tech. Symp.*, Jun. 2007, pp. 1471–1474.